Chapter 2. SCIIB Sensor Principle

The self-calibrated interferometric/intensity based (SCIIB) sensor technology is originated from the well-developed extrinsic Fabry-Perot interferometric (EFPI) fiber optic sensors. Ever since Fabry and Perot proposed and successfully demonstrated their famous concept of interferometry in 1898 [34], this interferometric principle has seen numerous practical applications. Fabry-Perot interferometers made of bulk optical components have been successfully applied to high precision measurement, optical spectrum analysis, optical wavelength filtering, and construction of lasers. However, due to the strict requirement of the alignment between the two optical surfaces in a Fabry-Perot interferometer, most Fabry-Perot interferometers based on bulk optics can only maintain their stability in laboratory environments. The convergence of optical fiber greatly easies the requirement of alignment in constructing Fabry-Perot interferometers, making fiber optic Fabry-Perot interferometers much more stable. Early research work on fiber optic Fabry-Perot interferometric sensors can be traced back to the mid 70s when Christensen at the Washington University successfully demonstrated multimode fiber based Fabry-Perot temperature sensors [35]. Thereafter, fiber optic Fabry-Perot sensors were developed into various structures and applied to the measurement of a wide variety of physical and chemical parameters [36-38].

The self-calibrated interferometric/intensity-based (SCIIB) fiber optic sensor successfully combines the advantages of both the interferometric and the intensity-based fiber sensors in a single system. Through a proper design of the sensor, the SCIIB technology can provide absolute measurement of various parameters with the full self-compensation capability for the source power fluctuation and the fiber loss changes. Starting with a review of fiber optic Fabry-Perot sensing techniques, this chapter will present the configuration of the SCIIB system followed by the detailed discussion of the unique signal processing method that offers the system self-calibration capability.

2.1 Review of Fiber Optic Fabry-Perot Sensors

Based on the construction of the Fabry-Perot cavities, fiber optic Fabry-Perot sensors can be categorized into two types including intrinsic sensors and extrinsic sensors. The intrinsic Fabry-Perot interferometric (IFPI) fiber optic sensor has a Fabry-Perot cavity constructed by a section of fiber with its two endfaces cleaved and coated with reflective coatings, while extrinsic Fabry-Perot interferometers have an interferometric cavity outside the fiber, and the fiber is only acting as a medium to transmit light into and out of the Fabry-Perot cavity.

2.1.1 IFPI sensor

As shown in Figure 2-1, an IFPI sensor is usually fabricated by splicing a section of fiber with its two endfaces coated with reflective films to a regular fiber. TiO_2 films with typical thickness of 40-80 nm are the common choice to form reflective coatings at the fiber endfaces with different reflectivity [39,40].

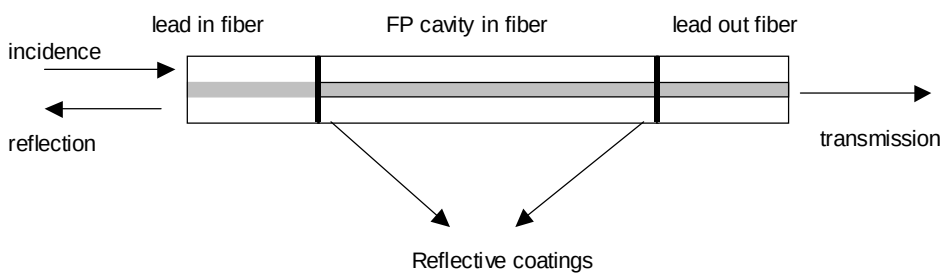

Figure 2-1. Illustration of an IFPI fiber optic sensor

The interferometric superposition of multiple reflections at the two fiber endfaces forms the output signal, which is a function of the fiber cavity length, the reflectance of the coating, and the refractive index of the fiber. The change of the cavity length or the refractive index of an IFPI sensor can be detected by monitoring the interference output

(either through the reflection or the transmission), thus, various physical or chemical parameters can be measured with a high resolution.

Temperature measurement is the most successful application of the IFPI sensors. Because a long section of fiber can be used to make the Fabry-Perot cavity, the sensitivity of temperature measurement can be very high, smaller than 0.01°C as reported in the literature [41]. Although in principle, the IFPI sensor can be used to measure parameters other than temperature such as pressure and strain [42-45], the experimental results indicated that IFPI sensors are not the best choice because of the large temperature cross coupling in the practical applications. Up to date, sensor structures or signal processing methods that can effectively eliminate the temperature cross coupling of an IFPI sensor have not been reported yet in publications.

It is worth to point out that intrinsic Fabry-Perot interferometers have successfully found their position in the world of fiber optic communications [46-49]. Intrinsic Fabry-Perot interferometers with a very high finesse can be used as in-line tunable filters in WDM systems to select a wavelength channel. Those tunable filters have the advantages of a low insertion loss, a larger tunable spectrum range, and a high spectrum resolution.

2.1.2 EFPI Sensor

As shown in Figure 2-2, a typical EFPI cavity can be formed by the air gap between two optical reflective surfaces. Although the two reflectors forming the Fabry-Perot cavity can be the surfaces of any optical components, a very simple way of forming an EFPI will be directly using the cleaved endfaces of two fibers.

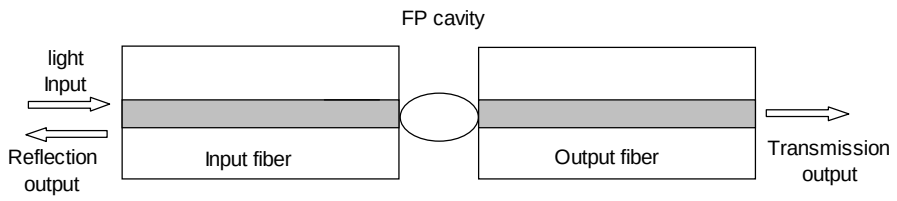

Figure 2-2. Illustration of an EFPI fiber optic sensor

Similar to the IFPI, the output interference signal form an EFPI is a function of the cavity length, and refractive index of the medium inside the Fabry-Perot cavity, and the reflectivity of the coatings of the two reflectors. Extrinsic Fabry-Perot interferometers can be used as sensors by monitoring the interference signals. Unlike the IFPI, the phase of the interference signal from an EFPI is independent of the input or output fiber, and more importantly it offers the flexibility to design the Fabry-Perot cavity to accommodate different applications. In general, EFPI fiber optic sensors have such advantages as high sensitivity, small size, simple structure, polarization independence, and great design flexibility. These have made extrinsic Fabry-Perot interferometers a better choice in many sensing applications. EFPI fiber optic sensors can be found in a wide variety of sensing applications to measure various physical or chemical parameters such as displacement [50-52], temperature [53-57], strain [58-69], pressure [24, 70-72], acoustic waves [73-76], and flow [77,78].

2.1.3 Review of Signal Processing Methods for EFPI Sensors

The simplest signal processing method for the EFPI sensors is direct interference fringe counting, which has been the dominant signal processing method in early EFPI sensors. However, due to the nonlinear and periodic nature of the sinusoidal interference fringes, the fringe counting method suffers from the problems such as sensitivity reduction when the sensor reaches peaks or valleys of the fringes, and fringe direction ambiguity, which practically limited the accuracy of measurement. Proposed by Murphy at al., it was

possible to count fringes bi-directionally by using a quadrature-phase-shifted two-interferometer structure [79]. However, it was also found difficult to maintain the exact phase difference between these two interferometers in practical applications.

More recently, several signal processing methods that have been successfully developed for other types of fiber interferometers were reported being used in EFPI sensors. Jackson(1988) [80], Hogg(1991) [81], Steward(1998) [82], and Gangopadhyay(1999) [83] reported their research on applying laser wavelength modulation based heterodyne interferometry to demodulate the interference signal of EFPI sensors. However, due to the short initial cavity length of the EFPI sensors, the resolution of the wavelength modulation based signal processing method was limited.

The whitelight scanning interferometry has also been used for EFPI sensors [51,84]. The system complexity was increased dramatically by using a second interferometer with its optical path difference scanned to match the optical path difference of the EFPI sensor. In addition, because mechanical scanning devices were used in most systems, the frequency response of the measurement was limited to the highest speed of the scanning devices, and the system stability could be a potential problem.

Lo (1996) [85], Furstenau(1998) [86], and Schemidt(1999) [87] reported using multiple wavelengths to interrogate the EFPI cavity length. The dynamic range of the measurement was increased because the effective wavelength of this technique becomes the beat wavelength of the multiple sources, which is much larger than that of a single source. However, the stability problem of the sensor became worse because the wavelengths of the multiple sources could drift in different directions.

In summary, more than 20 years of research on EFPI fiber optic sensors have brought dramatic progresses in the EFPI sensor structure design and broadened their application areas. However, summarizing the research work reported in literatures, effective signal

processing methods are still not available for EFPI sensors. This situation mainly results from the following reasons. First, EFPI sensors usually have a very short initial cavity length, which makes the wavelength modulation based heterodyne interferometry difficult to apply. Second, in the EFPI sensor structure, unlike the Mickelson interferometer or the Mach-Zehnder interferometer, the reference path and the signal path of an EFPI sensor are packed together. In real applications, the reference path is unreachable, which makes it difficult to modulate the reference optical path so that phase modulation based interferometry becomes very difficult. Third, effective methods that can compensate the source power drifting and fiber loss variations are not available, which can result in a large measurement error when the signal processing methods based on intensity detection are directly applied.

2.2. SCIIB System Configuration

The basic configuration of the SCIIB fiber sensor system can be illustrated using Figure 2-3. The system includes a sensor probe, a broadband source, an optoelectronic signal processing unit and silica glass fibers linking the sensor probe and the signal-processing unit.

The light from the broadband optical source (for example an LED) is launched into a two-by-two fiber coupler through the pigtailed fiber, and propagates along the optical fiber to the sensor head. The sensor head is constructed by inserting two optical fibers, with their endfaces cleaved, into a capillary tube so that an air-gapped low finesse Fabry-Perot cavity is formed between the two fiber endfaces, as shown in the enlarged view of the sensor head. The incident light is first partially reflected (~4%) at the endface of the input fiber. The remainder of the light propagates across the air gap to the endface of the reflector fiber, where a second reflection (~4%) is generated. The two reflections then travel back along the same fiber and through the same fiber coupler to the signal-

processing unit. The signal processing part of the SCIIB system extracts the information about the Fabry-Perot cavity length, which is related to various measurands governed by different physical laws.

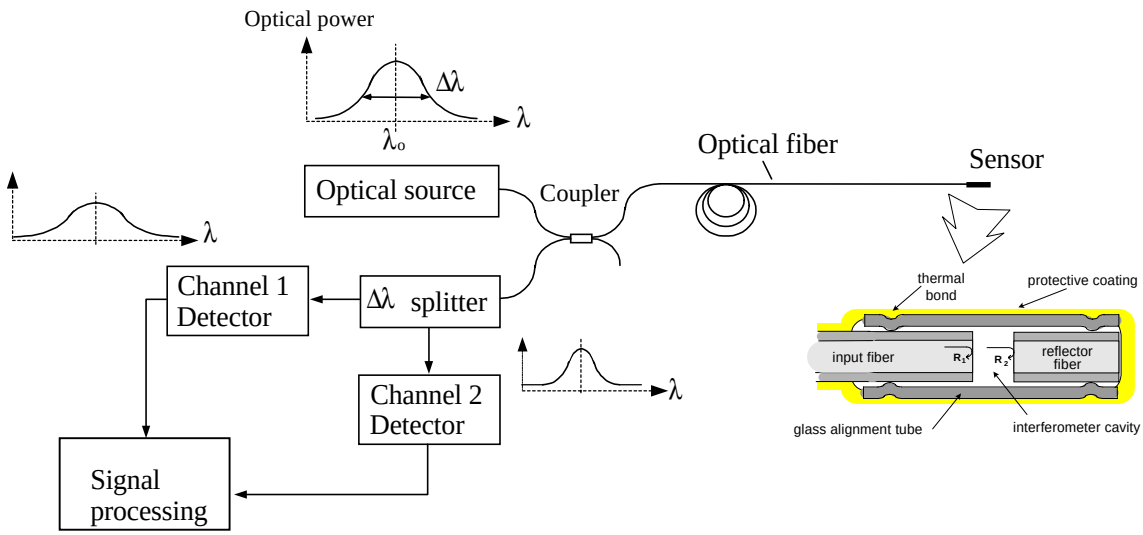

Figure 2-3. Illustration of the principle of SCIIB fiber optic sensor system

2.3 SCIIB Signal Processing

From the theories of optics, we know that the coherence length of a source is inversely proportional to the spectral width of the source. The coherence length L_c can be estimated by the following formula

$$L_c \approx \frac{\lambda_c^{\ 2}}{\Delta\lambda}, \tag{2-1}$$

where λ_c is the central wavelength of the source and $\Delta\lambda$ is the spectral width of the source. To obtain an interference signal from the interferometer, the optical path difference (OPD) has to be smaller than the coherence length of the source. If the OPD of the interferometer is larger than the coherence length of the source being used, the two optical waves will not effectively interfere to generate fringes.

As shown in Figure 2-3, the reflected light from the sensor head is split into two channels with different optical properties through optical filtering. The light in Channel 1 retains its original spectral width (broadband spectrum) while the light in Channel 2 has a narrower spectrum by passing it through an optical bandpass filter. The different spectral widths of the light result in different coherence lengths of these two channels.

Let's study the two channel output signals in terms of optical interference. First, Let's assume that the original spectrum of the source can be approximated as a Gaussian profile with a spectral width of $\Delta\lambda_1$, and also assume that the spectral characteristic of the optical bandpass filter is a Gaussian profile too, but with a different spectral width of $\Delta\lambda_2$. The light spectra seen by the two SCIIB channels can thus be expressed by

$$I_{s1.s2}(\lambda) = \frac{2I_{10,20}}{\sqrt{\pi}\Delta\lambda_{1,2}} \exp\left(-\frac{(\lambda - \lambda_c)^2}{\Delta\lambda_{1,2}{}^2} \right), \tag{2-2}$$

where $I_{10,20}$ are the optical powers of the two channels respectively, and λ_c is the central wavelength for both channels (here, we assume that the two channels have the same central wavelength).

If we neglect the multiple reflections, the interference signals resulting from the spectra of the two channels can thus be written as

$$I_{1,2} = R \cdot \int_0^\infty I_{s1,s2}(\lambda)[1 + \eta^2 (1-R)^2 - 2\eta(1-R)\cos(\frac{4\pi}{\lambda}L)]d\lambda\,, \tag{2-3}$$

where

- $I_{s1,s2}$ are the spectral power density distribution of the two channels respectively
- R is the reflectance at the boundary of the air and the fiber endface
- L is the cavity length

- η is the coupling coefficient of the Fabry-Perot cavity. It is a function of the cavity length *L*, the lateral offset, and the angular offset. Because the initial cavity length usually is chosen to be very small, the optical loss of the cavity is very small. Therefore, η can be approximated to 100%.

The reflectance *R* can be calculated by

$$R = [\frac{(n-n')}{(n+n')}]^2 , \tag{2-4}$$

where *n* is the refractive index of the fiber core, and *n'* is the refractive of the medium forming the cavity between two fibers, which in our case is the air. The reflectance at the fiber endfaces is thus about 4% of the total incident optical power.

Notice that the reflectance is relatively small, the interference signals given by Equation (2-3) can thus be approximated by

$$I_{1,2} \approx 2R \cdot \int_0^{\infty} I_{s1,s2}(\lambda)[1-\cos(\frac{4\pi}{\lambda}L)]d\lambda . \tag{2-5}$$

Equation (2-5) indicates that the interference signal is the superposition of interference contribution of all the spectral components. Here we have assumed that the photodetectors have a flat response over the source emission spectrum.

By taking the ratio of the two channels outputs, we then have the SCIIB output given by

$$s = \frac{I_2}{I_1} \approx \frac{\int_{-\infty}^{\infty} I_{s2}(\lambda)[1-\cos(\frac{4\pi}{\lambda}L)]d\lambda}{\int_{-\infty}^{\infty} I_{s2}(\lambda)[1-\cos(\frac{4\pi}{\lambda}L)]d\lambda} . \tag{2-6}$$

Figure 2-4 shows the output signals from the two SCIIB channels, and Figure 2-5 plots their ratio given by Equation (2-6) as the function of the sensor cavity length, where the source spectral width is assumed to be 40nm and that of the bandpass filter is 10nm, which corresponds to the single-mode fiber sensor case as we will discussed later. Figure

2-6 and Figure 2-7 show the similar simulation results for the case in accordance with the multimode fiber sensor system which uses a source with the spectral width of 70nm and the spectral width of the filter is 10nm.

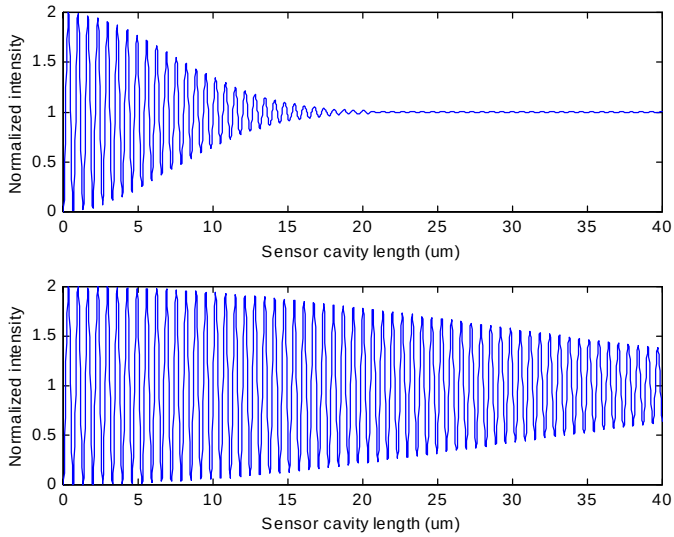

Figure 2-4. Interference fringes of the SCIIB two channels, where the source has the spectral width of 40nm and the central wavelength of 1310nm; the spectral width of the bandpass filter is 10nm, in accordance with the single-mode fiber sensor system.

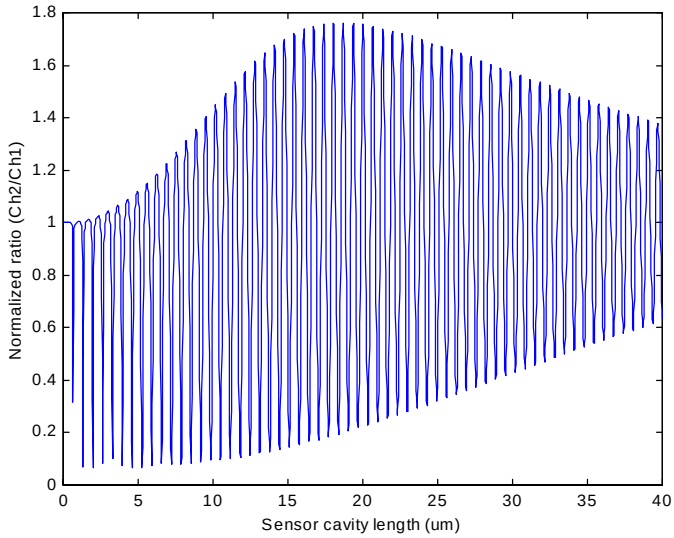

Figure 2-5. Ratio of the two channels' outputs of Figure 2-4

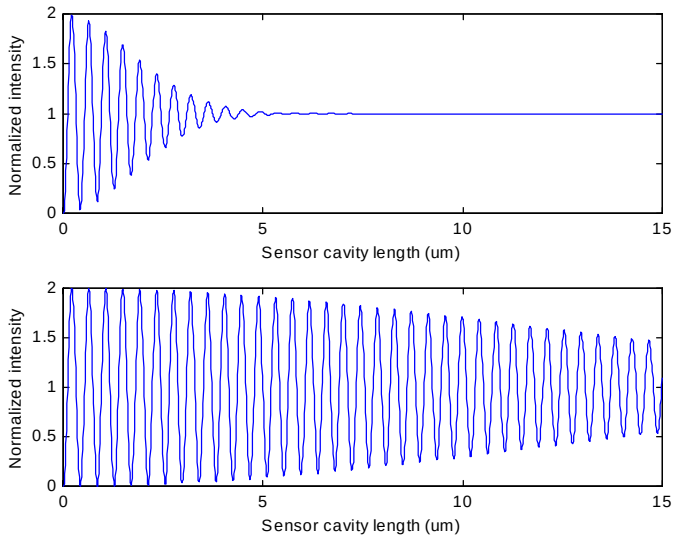

Figure 2-6. Interference fringes of the SCIIB two channels, where the source has the spectral width of 70nm and the central wavelength of 850nm; the spectral width of the bandpass filter is 10nm, in accordance with the multimode fiber sensor system.

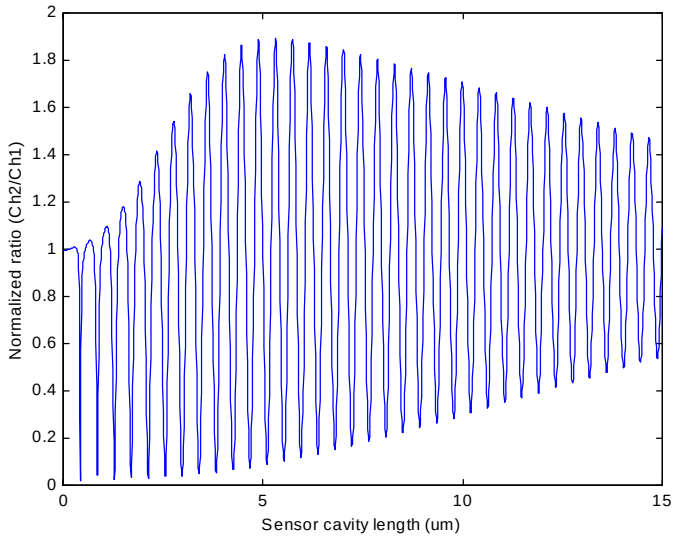

Figure 2-7. Ratio of the two channels' outputs of Figure 2-6

If we fabricate the sensor probe in such a way that it has an initial cavity length that is larger than the coherence length of Channel 1 but smaller than the coherence length of

Channel 2, then, as shown in Figure 2-4 and 2-6, Channel 1 becomes an intensity channel with its output relatively unchanged, while Channel 2 retains its highly visible interference fringes as the cavity length changes.

The output from Channel 1 (non-interference channel) and Channel 2 (interference channel) of the SCIIB sensor can now be expressed as

$$I_1 \approx 2RI_{10}, \tag{2-7}$$

and

$$I_2 = 2R \cdot I_{10} \cdot \alpha \cdot [1 - \gamma \cos(\frac{4\pi}{\lambda} L)], \tag{2-8}$$

where, α is the power loss of the optical filter in Channel 2, given by

$$\alpha = \frac{I_{20}}{I_{10}}, \tag{2-9}$$

and γ is the fringe visibility of Channel2's signal, which is defined by

$$\gamma = \frac{I_{\max} - I_{\min}}{I_{\max} + I_{\min}}, \tag{2-10}$$

where, I_{max} and I_{min} is the maximum and minimum intensity of the optical interference respectively. The fringe visibility in our case is a function of η, R, and $\Delta\lambda_2$.

In principle, continuously tracking the phase change of the interference fringes in Channel 2 would permit measurement of the change of the cavity length of the sensor head. Like the output of a regular interferometer, the measurement will have ultra-high sensitivity. One period of fringe variation corresponds to an air gap change of one-half of the optical wavelength. However, the fiber loss variations and the laser power drift could introduce errors to the amplitude of the interference signal and result in a poor accuracy of the measurement. To avoid these two adverse effects, we introduce the output from Channel 1 to the signal processing as a reference signal, and the SCIIB sensor output is evaluated as the ratio of the two signals of the two channels, given by

$$s = \frac{I_2}{I_1} \approx \frac{2RI_{10}\alpha[1-\gamma\cos(\frac{4\pi}{\lambda}L)]}{2RI_{10}} = \alpha[1-\gamma\cos(\frac{4\pi}{\lambda}L)] \quad . \tag{2-11}$$

The two channel signals are from the same source and experience the same transmission paths. They thus have similar behaviors in terms of source power fluctuation and fiber loss variations. As indicated in Equation (2-11), the ratio of the outputs from Channel 2 and Channel 1 is only a function of the Fabry-Perot cavity length, which can thus eliminate these two sources of errors from the final result of the measurement.

To assure the proper self-referencing function of the SCIIB sensor system, it is very important to choose an optimal initial sensor cavity length that gives the signal channel maximum fringe visibility and at the same time the interference of the reference channel is suppressed to minimum. The choice of the optimal initial cavity length will mainly depend on the spectral widths of the two SCIIB channels. For example, in the case shown in Figure 2-4 and 2-5, the initial cavity length can be chosen between 20 and 30μm. On the other hand, for the case shown in Figure 2-6 and 2-7, the initial cavity length can be somewhere from 7 to 12μm. However, there are other considerations in determining an optimal initial cavity length, which will be further studied later in Chapter 6.

2.4 Linear Operating Range of SCIIB Sensor

Regular interferometric sensors suffer from the disadvantages of sensitivity reduction and the fringe direction ambiguity when the sensor output reaches the peak or valley of an interference fringe. Sensitivity is reduced at the peak or valley of a fringe since at that point the change in optical intensity is zero for a small change in the sensor cavity length. Fringe direction ambiguity refers to the difficulty in determining from the optical

intensity whether the sensor cavity is increasing or decreasing. To avoid these two problems, we design and fabricate the SCIIB sensor head to operate only over the semi-linear range of a half fringe, as shown in Figure 2-8, so that a one-to-one quantitative relation between output intensity and the sensor cavity length is obtained.

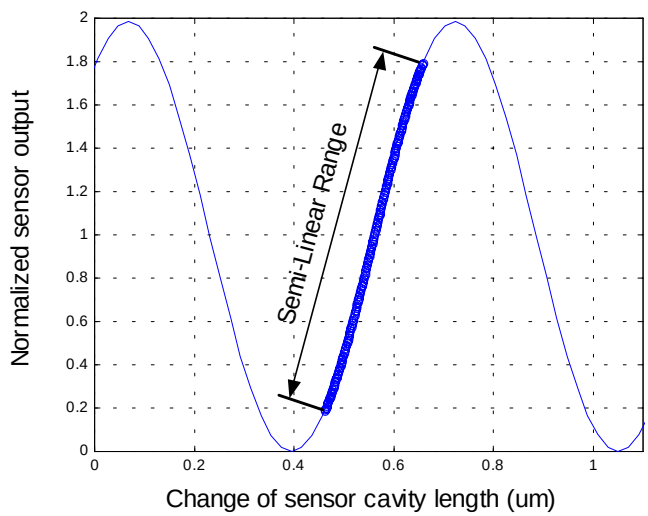

Figure 2-8. Illustration of a semi-linear operating range of fringes.

We define the linear range of the SCIIB sensor based on the change of its sensitivity. From Equation (2-11), the sensitivity of the SCIIB sensor can be calculated by

$$Sensitivity = abs(\frac{ds}{dL}) = abs(\alpha\gamma \frac{4\pi}{\lambda} \sin(\frac{4\pi}{\lambda} L)) . \tag{2-12}$$

The maximum sensitivity is obtained at the Quadrature (Q)-points of the interference fringes, which is

$$Maximum \quad Sensitivity = \alpha\gamma \frac{4\pi}{\lambda} . \tag{2-13}$$

Correspondingly, we define the operating range of the SCIIB sensor as its sensitivity remaining within 60% of the maximum sensitivity. Therefore the operating range can be calculated by

$$\{Operating \quad Range\} = Solution\{abs(\alpha\gamma \frac{4\pi}{\lambda} \sin(\frac{4\pi}{\lambda} L)) \leq \gamma \frac{4\pi}{\lambda} \cdot 60\%\}, \qquad (2\text{-}14)$$

which results in the maximum change of the signal level Δs given by

$$\Delta s_{\max} = 1.6\alpha\gamma . \qquad (2\text{-}15)$$

2.5. Major Advantages of the SCIIB Sensor Technology

In addition to the generic fiber sensor advantages such as small size, lightweight, remote operation, immunity to EMI, electrically non-conducting, and chemical inertia, the unique SCIIB signal processing method combines the advantages of both interferometric and intensity-based sensors and provides the sensor a number of other major advantages as summarized as below:

1. Ultra-high sensitivity.

The SCIIB fiber optic sensor can offer a very high resolution to the measurement since the essence of the signal processing is based on interferometry.

2. Absolute measurement.

The operating range of the SCIIB sensor is limited to the semi-linear range of half of an interference fringe; therefore the sensor output is a unique and almost linear function of the change of the cavity length. The one-to-one relation between the sensor output and the cavity length makes it possible to measure the absolute value of the sensor cavity length after the initial cavity length is chosen and fixed. Not only the direction ambiguity problem is solved, but also the sensitivity of the sensor is kept relatively constant during the entire operating range.

3. Minimized complexity in signal processing.

Because the signal processing of the SCIIB sensor only involves optical power detection and a simple ratio operation of the two output signals, the complexity of the system is then kept to a minimum level.

4. Self-compensation capability.

Since the original broadband source spectrum is used as a reference signal, the drift of source power and fluctuations in fiber attenuation are thus fully compensated by the SCIIB signal processing.

5. High frequency response.

Because the very simple signal processing is used, the SCIIB sensor potentially has a very high frequency response, which may allow the detection of very high-speed signals such as acoustic waves or aerodynamic forces.

6. Geometric flexibility.

The Fabry-Perot sensor head structure can also offer a great design flexibility to accommodate the requirements for different applications.